Theor Chem Account (2009) 122:207–216
DOI 10.1007/s00214-008-0500-1

REGULAR ARTICLE

Theoretical mechanistic study on the radical-molecule reaction of $CH_2Br/CHBrCl$ with NO_2

Xiu-Juan Jia · Xiu-Mei Pan · Jing-Yu Sun · Yi-Zhen Tang · Hao Sun · Ya-Ru Pan · Rong-Shun Wang

Received: 10 September 2008 / Accepted: 10 December 2008 / Published online: 30 December 2008

Abstract The radical-molecule reaction mechanisms of CH_2Br and CHBrCl with NO_2 have been explored theoretically at the UB3LYP/6-311G(d, p) level. The single-point energies were calculated using UCCSD(T) and UQCISD(T) methods. The results show that the title reactions are more favorable on the singlet potential energy surface than on the triplet one. For the singlet potential energy surface of $CH_2Br + NO_2$ reaction, the association of CH_2Br with NO_2 is found to be a barrierless carbon-to-oxygen attack forming the adduct IM1 ($H_2BrCONO$-trans), which can isomerize to IM2 (H_2BrCNO_2), and IM3 ($H_2BrCONO$-*cis*), respectively. The most feasible pathway is the 1, 3-Br shift with C–Br and O–N bonds cleavage along with the N–Br bond formation of IM1 lead to the product P1 ($CH_2O + BrNO$) which can further dissociate to give P4 ($CH_2O + Br + NO$). The competitive pathway is the 1, 3-H-shift associated with O–N bond rupture of IM1 to form P2 (CHBrO + HNO). For the singlet potential energy surface of $CHBrCl + NO_2$ reaction, there are three important reaction pathways, all of which may have comparable contribution to the reaction of CHBrCl with NO_2. The theoretically obtained major products CH_2O and CHClO for $CH_2Br + NO_2$ and $CHBrCl + NO_2$ reactions, respectively, are in good agreement with the kinetic detection in experiment.

Keywords Reaction mechanism · Potential energy surface · Bromomethyl (CH_2Br) · Bromochloromethyl (CHBrCl) · Nitric dioxide (NO_2)

1 Introduction

Nitrogen oxides, known to be the major atmospheric pollutants released by combustion process, have attracted extensive attentions both experimentally and theoretically. In order to minimize the harmful effects before their release in the atmosphere, one effective way is to reduce them chemically by their reactions with other species [1–4]. Several halogenated methanes (CH_3Br, CH_3I, CH_2I_2, CH_2IBr, CH_2ICl, CH_2Br_2, $CHBr_3$ etc.) have been observed on coastal and pelagic ocean areas [5]. The natural source of bromomethane has been found to be a marine phytoplankton [6]. Bromomethane is considered to be the most abundant atmospheric source of bromine atoms, which have been considered to take a part in the catalytic destruction of ozone in the Earth's atmosphere. Bromomethane is a very toxic compound and it is used for methylation in organic synthesis and as a fumigant. Obviously, the main atmospheric precursor of the CH_2Br radical is bromomethane ($OH + CH_3Br \rightarrow CH_2Br + H_2O$) [7–9]. The reaction with OH has a principal loss process for atmospheric bromomethane. The CH_2Br radical may react further in exothermic reactions with other open shell species, such as H, O, hydrocarbon radicals, and NO_X ($X = 1, 2$) at atmospheric conditions to release Br atom for

Electronic supplementary material The online version of this article (doi:10.1007/s00214-008-0500-1) contains supplementary material, which is available to authorized users.

X.-J. Jia · X.-M. Pan (✉) · J.-Y. Sun · Y.-Z. Tang · H. Sun · Y.-R. Pan · R.-S. Wang (✉)
Faculty of Chemistry, Institute of Functional Material Chemistry, Northeast Normal University, 130024 Changchun, People's Republic of China
e-mail: panxm460@nenu.edu.cn

X.-J. Jia
e-mail: jiaxj753@nenu.edu.cn

R.-S. Wang
e-mail: wangrs@nenu.edu.cn

secondary reaction with ozone. The other product from this reaction is BrO which self-reaction produces molecular bromine and oxygen. A similar set of elementary reactions may be considered to occur for bromochloromethane. It has also considered as an effective fire suppressant. Both bromomethane as well as bromochloromethane have been detected at lower stratosphere among other brominated compounds [10]. In addition, atmospheric photolysis of dibromomethane ($CH_2Br_2 + hv \rightarrow CH_2Br + Br$) may also have some importance in producing CH_2Br radical in the upper troposphere and in the lower stratosphere [11]. Reactions with NO_2 can be expected to be important during the oxidation of halogenated compounds at low temperature, because traces of nitrogen oxides are also often present [12]. Due to their significance, several experimental and theoretical investigations on the reactions of halogenated alkyl radicals with NO_2 have been carried out [13–17].

Reliable information on the kinetics of these halogenated methyl radical reactions is of importance for the modeling of NO_x-involved reaction processes. Recently, Timonen et al. [14] reported for the first time the rate constants of the $CH_2Br + NO_2$ and $CHBrCl + NO_2$ reactions over the temperature ranges (220–360 K) using a laser photolysis/photoionization mass spectrometry and derived the rate constant expression as $(1.76 \pm 0.03) \times 10^{-11}$(T/300 K) $- 0.86 \pm 0.09$ and $(8.81 \pm 0.28) \times 10^{-12}$ (T/300 K) $- 1.55 \pm 0.34$ cm^3 mol^{-1} s^{-1}, respectively. The observed products were CH_2O and CHClO, respectively. In addition, a week signal for NO formation has been detected for the reactions. However, the available information on product channels, product distributions, and reaction mechanism was not further provided though this information may be important in the NO_2-involved sequential chain processes. To our best knowledge, no theoretical study has been reported for the title reactions. In view of the potential importance and the rather limited information, we carry out a detailed theoretical study on the potential energy surface (PES) of the title reactions to (1) provide the elaborated isomerization and dissociation channels on the $H_2BrCONO$ and HBrClCONO PESs; (2) investigate the products of the title reactions to assist in further experimental identification; (3) make comparisons between the reactions of CHBrX (X=H and Cl) with NO_2 to deeply understand the halogenated methyl chemistry.

2 Computational methods

All calculations are carried out using the GAUSSIAN 03 program packages [18]. The geometries of all the reactants, products, intermediates, and transition states are optimized using the hybrid density functional UB3LYP method (Becke's three parameter hybrid functional with the nonlocal correlation functional of Lee–Yang–Par) [19, 20] with 6-311G(d, p) basis set. The stationary nature of structures is confirmed by harmonic vibrational frequency calculations, i.e., equilibrium species possess all real frequencies, whereas transition states possess one and only one imaginary frequency. The zero-point energy (ZPE) corrections are obtained at the same level of theory. In order to obtain more reliable energetic data, higher level single-point energy calculations are performed at UCCSD(T)/6-311G(d, p) and UQCISD(T)/6-311G(d, p) [21] by using the UB3LYP/6-311G(d, p) optimized geometries. To confirm that the transition states connect designated intermediates, intrinsic reaction coordinate (IRC) calculation [22, 23] is carried out at the UB3LYP/6-311G(d, p) level of theory. Moreover, unless otherwise specified, the UCCSD(T) single-point energies with ZPE corrections are used in the following discussions.

3 Results and discussion

The optimized structures of important stationary points as well as the corresponding experimental values [24, 25] for the two reactions are depicted in Figs. 1 and 2, respectively. By means of the transition states and their connected products, the schematic PESs for the two reactions in singlet are plotted in Figs. 3 and 4, respectively. The harmonic vibrational frequencies of important stationary points including available experimental values [26] are listed in Tables 1 and 2, respectively. Note that the calculated geometries and frequencies at the UB3LYP/6-311G(d, p) level are in good agreement with experimental results. The ZPE corrections and relative energies for the most relevant species are summarized in Tables 3 and 4. It is shown that relative energies at UCCSD(T)//UB3LYP/6-311G(d, p) and UQCISD(T)//UB3LTP/6-311G(d, p) levels are in good accordance. To make our discussion easier, the total energy of the reactants R for each reaction is set to be zero for reference. For the two reactions, the reactant molecules are doublet and the spin contamination is not severe; i.e., the $\langle S^2 \rangle$ values of CH_2Br, CHBrCl and NO_2 are less than 0.76, very close to the expected values of the pure double states 0.75. The total energy of the reactant system was obtained by addition of the energies of the doublet molecules for the title reactions.

3.1 Reaction $CH_2Br + NO_2$

3.1.1 Initial association

Both singlet and triplet CH_2BrNO_2 potential energy surfaces (PESs) have been obtained for the radical-molecule reaction of CH_2Br (C_{2v}, $^2B1$) + NO_2 (C_{2v}, $^2A1$). With the

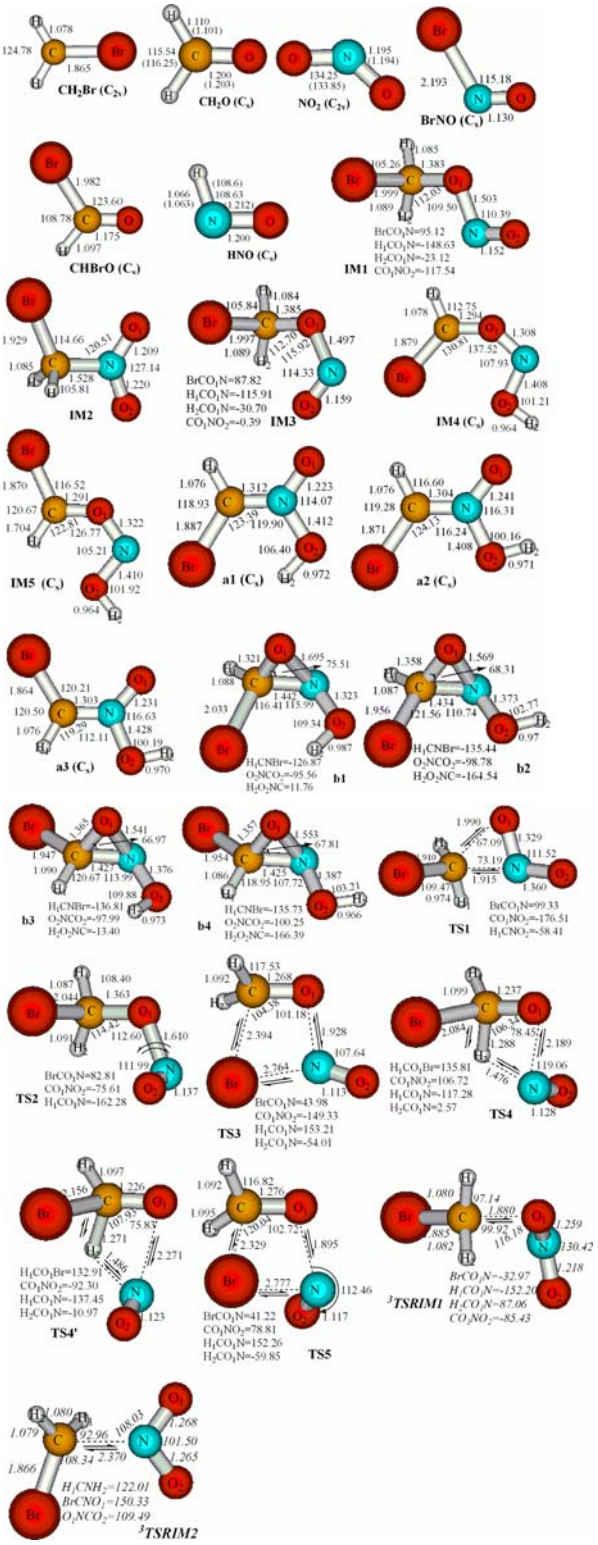

Fig. 1 The UB3LYP/6-311G(d, p) optimized geometries of reactants, some important products, isomers, and transition states for $CH_2Br + NO_2$ reaction. The values in *italics* are for the triplet species. The values in parentheses are the experimental values ([24] for NO_2, CH_2O, [25] for HNO). In the transition states the direction of the imaginary frequency is indicated by " $\rightleftharpoons$ ". Bond distances are in angstroms and angles are in degrees

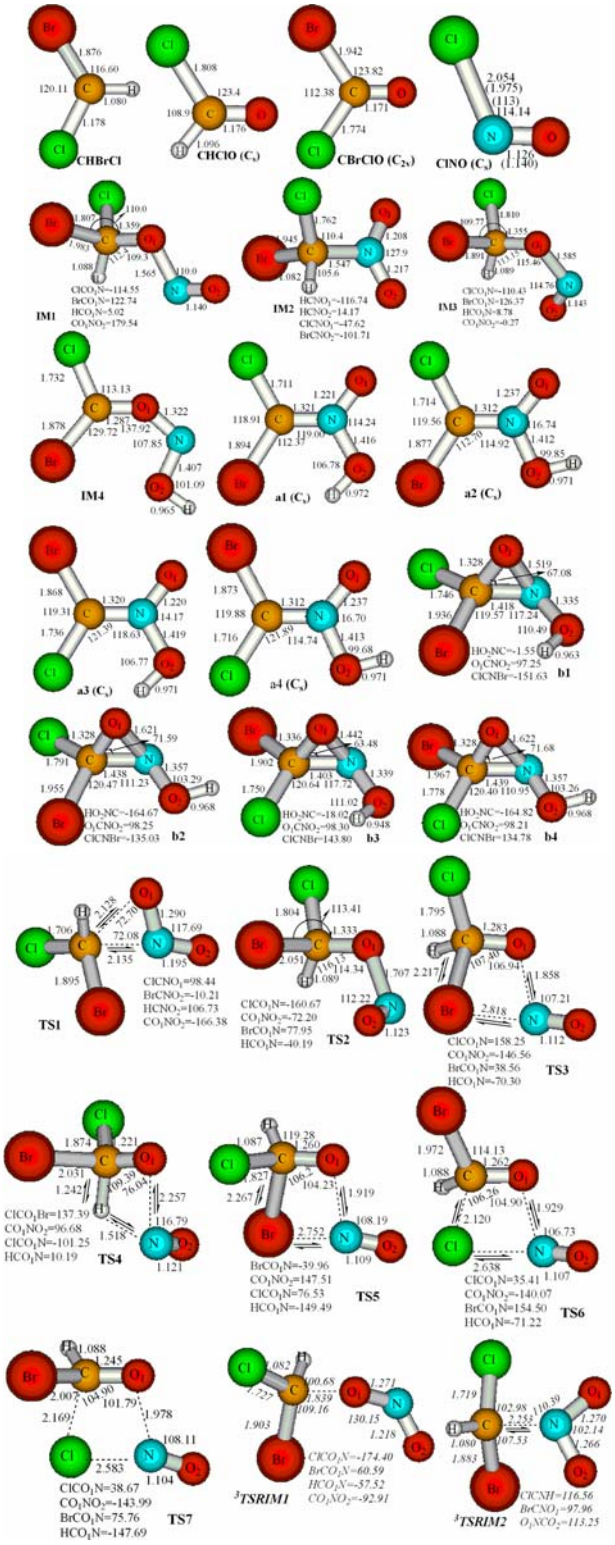

Fig. 2 The UB3LYP/6-311G(d, p) optimized geometries of reactants, some important products, isomers, and transition states for $CHBrCl + NO_2$ reaction. The values in italics are for the triplet species. The values in parentheses are the experimental values [25] for ClNO). In the transition states the direction of the imaginary frequency is indicated by " $\rightleftharpoons$ ". Bond distances are in angstroms and angles are in degrees

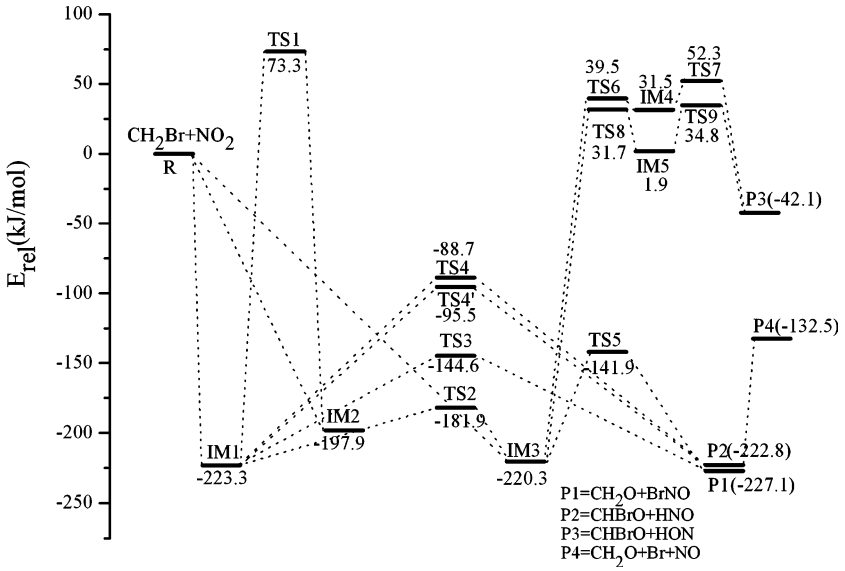

Fig. 3 Schematic singlet potential energy surface of the reaction channels for the $CH_2Br + NO_2$ reaction at the UCCSD(T)//UB3LYP/6-311G(d, p) + ZPE level. E_{rel} are the relative energies (kJ/mol)

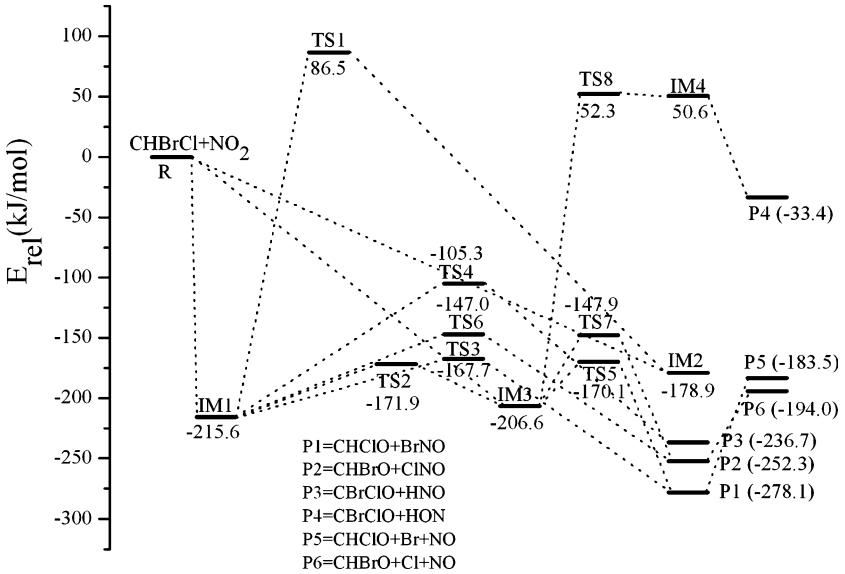

Fig. 4 Schematic singlet potential energy surface of the reaction channels for the $CHBrCl + NO_2$ reaction at the UCCSD(T)//UB3LYP/6-311G(d, p) + ZPE level. E_{rel} are the relative energies (kJ/mol)

different atom (N or O atom) in NO_2 approaching to C atom, different intermediates are formed, namely, IM1 ($H_2BrCONO$-*trans*), IM2 (H_2BrCNO_2) and IM3 ($H_2BrCONO$-*cis*), respectively. The association is expected to be fast and will play a significant role in the reaction kinetics. On the singlet PES, the carbon-to-oxygen approach is more attractive to form structures IM1 and IM3 without any encounter barrier than to form the carbon-to-nitrogen approach intermediate IM2. The intermediates IM1 and IM3 are located as two energy minima lying 223.3 and 220.3 kJ/mol below the reactants R, and also lying 25.4 and 22.4 kJ/mol lower than IM2 (C_s, $^1A'$), respectively. Therefore, from the energy point of view, IM1 and IM3 could be initially formed and this reaction is most likely to be initiated by the carbon-to-oxygen approach on the singlet PES. Furthermore, IM1 can isomerize to IM2 via the transition state TS1, as shown in Fig. 3. On the other hand, there is a substantial barrier of 95.3 kJ/mol (^{3}TSRIM1) for the carbon-to-oxygen attack on the triplet PES to form ^{3}IM1 (7.8 kJ/mol) and the carbon-to-nitrogen approach can lead to the triplet isomer ^{3}IM2 (−40.8 kJ/mol) via the transition state ^{3}TSRIM2 with much higher barrier of 177.9 kJ/mol. In view of the much higher entrance barriers, the triplet pathways may contribute less to the $CH_2Br + NO_2$ reaction compared with the singlet pathways, and thus will not be further discussed. In the following discussions, we mainly discuss the formation pathways of various products proceeding via intermediate IM1.

Table 1 UB3LYP/6-311G(d, p) harmonic vibration frequencies (cm^{-1}) and experimental values of reactant, some important products, isomers, and transition states for $CH_2Br + NO_2$ reaction

Species	UB3LYP	Expt[a]
CH_2Br	89, 696, 930, 1,382, 3,169, 3,328	
NO_2	766, 1,399, 1,707	750, 1,318, 1,618
CH_2O	1,202, 1,270, 1,539, 1,825, 2,870, 2,920	
BrNO	271, 555, 1,942	190, 350, 365.5, 1816.2, 1820.0
CHBrO	347, 627, 909, 1,293, 1,877, 3,038	646.3, 893.4, 1270.9, 1797.9, 1799.9, 2911.9
HNO	1,576, 1,673, 2,830	1,511, 1,569, 2,854
NO	1,988	1,904
IM1	71, 215, 328, 378, 458, 612, 827, 938, 1,031, 1,256, 1,301, 1,457, 1,794, 3,094, 3,189	
IM2	77, 179, 273, 340, 502, 596, 759, 932, 1,108, 1,267, 1,302, 1,468, 1,849, 3,092, 3,183	
IM3	39, 196, 375, 571, 655, 736, 899, 910, 1,209, 1,282, 1,395, 1,438, 1,672, 3,127, 3,205	
TS1	719i, 82, 131, 264, 343, 563, 723, 783, 1,043, 1,120, 1,209, 1,384, 1,633, 3,177, 3,320	
TS2	222i, 81, 217, 303, 371, 554, 730, 907, 1,078, 1,246, 1,278, 1,476, 1,902, 3,059, 3,157	
TS3	234i, 146, 174, 259, 331, 402, 547, 741, 1,091, 1,209, 1,376, 1,544, 2,042, 3,033, 3,125	
TS4	640i, 73, 198, 225, 366, 389, 566, 682, 1,035, 1,157, 1,247, 1,527, 1,698, 2,013, 3,021	
TS5	187i, 121, 159, 265, 300, 469, 580, 789, 1,100, 1,208, 1,345, 1,537, 2,008, 3,012, 3,109	

[a] Experimnetal values from Ref. [26]

Table 2 UB3LYP/6-311G(d,p) harmonic vibration frequencies (cm^{-1}) and experimental values of reactant, some important products, isomers, and transition states for $CHBrCl + NO_2$ reaction

Species	UB3LYP	Expt[a]
CHBrCl	245, 438, 662, 831, 1,223, 3,220	866, 1,196
CHClO	441, 708, 945, 1,327, 1,873, 3,056	306.3, 633.6, 779.5, 1153.8
CBrClO	236, 365, 501, 547, 764, 1,899	240, 374, 517, 547, 806, 1,828
ClNO	318, 592, 1,967	323, 596, 1,800
IM1	50, 170, 197, 216, 253, 338, 548, 647, 707, 773, 1,126, 1,210, 1,341, 1,909, 3,121	
IM2	31, 168, 208, 257, 397, 608, 681, 758, 826, 884, 1,216, 1,256, 1,377, 1,680, 3,201	
IM3	27, 178, 199, 237, 253, 357, 517, 662, 707, 834, 1,064, 1,212, 1,357, 1,872, 3,103	
TS1	684i, 59, 91, 159, 252, 278, 376, 541, 749, 836, 960, 1,183, 1,247, 1,620, 3,264	
TS2	204i, 44, 130, 200, 228, 297, 500, 565, 661, 741, 1,117, 1,196, 1,316, 1,985, 3,092	
TS3	188i, 63, 139, 194, 236, 284, 461, 474, 585, 736, 1,086, 1,292, 1,304, 2,045, 3,110	
TS4	354i, 61, 177, 195, 241, 297, 383, 437, 614, 650, 773, 1,207, 1,530, 1,759, 2,031	
TS5	208i, 77, 152, 202, 251, 306, 416, 454, 568, 695, 1,016, 1,278, 1,367, 2,066, 3,136	
TS6	253i, 61, 143, 199, 209, 303, 405, 458, 552, 656, 1,080, 1,271, 1,362, 2,078, 3,110	

[a] Experimnetal values from Ref. [26]

3.1.2 Isomerization and dissociation pathways

The initial adduct IM1 is a stable chain-like intermediate lying 223.3 kJ/mol below the reactants. As shown in Fig. 3, the intermediate IM1 can isomerize to another chain-like intermediate IM2 undergoing the C–N bond formation along with C–O_1 bond rupture via TS1 as shown in Fig. 1, the transition state TS1 has a loose CNO1 three-membered ring structure, in which the length of forming C–O_1 bond is surprisingly long as 1.990 Å, while the C–N bond that will broken is 1.915 Å. The vibrational mode of frequency of TS1 corresponds to C–O and C–N bonds stretch vibration. The barrier height for this process is calculated to be 296.6 kJ/mol, which is very large to undergo. The conversion from IM1 ($H_2BrCONO$-*trans*) to IM3 ($H_2BrCONO$-*cis*) can be realized via O_1–N rotation transition state TS2 with small internal rotation barrier (41.3 kJ/mol above IM1). Subsequently, intermediate IM3 can dissociate to give the primary product P1 (CH_2O (C_{2v}, $^1A1$) + BrNO (C_s, $^1A'$) via TS5. Furthermore, the isomers IM1 and IM3 can directly dissociate to give product P1 via C–Br and N–O_1 bonds cleavage accompanied by N–Br bond formation

Table 3 ZPE Corrections (a.u.) and relative energies (kJ/mol) (including the UB3LYP/6-311G(d, p) zero-point energy (ZPE) corrections) of reactants, some important products, isomers, and transition states for the $CH_2Br + NO_2$ reaction at the UCCSD(T)//UB3LYP/6-311G(d, p) and UQCISD(T)//UB3LYP/6-311G(d, p) levels

Species	ZPE	UCCSD(T)//UB3LYP	UQCISD(T)//UB3LYP
R $CH_2Br + NO_2$	0.030686	0.0	0.0
P1 $CH_2O + BrNO$	0.032792	−227.1	−227.6
P2 $CHBrO + HNO$	0.032285	−222.8	−220.6
IM1	0.038570	−223.3	−223.1
IM2	0.040345	−197.9	−196.4
IM3	0.038611	−220.3	−220.2
TS1	0.035938	73.3	68.7
TS2	0.037269	−181.9	−181.1
TS3	0.036495	−144.6	−146.5
TS4	0.032107	−88.7	−89.4
TS5	0.036454	−141.9	−143.4

Table 4 ZPE corrections (a.u.) and relative energies (kJ/mol) (including the UB3LYP/6-311G(d, p) zero-point energy (ZPE) corrections) of reactants, some important products, isomers, and transition States for the $CHBrCl + NO_2$ reaction at the UCCSD(T)//UB3LYP/6-311G(d, p) and UQCISD(T)//UB3LYP/6-311G(d, p) levels

Species	ZPE	UCCSD(T)//UB3LYP	UQCISD(T)//UB3LYP
R $CHBrCl + NO_2$	0.023004	0.0	0.0
P1 $CHClO + BrNO$	0.025328	−278.1	−279.2
P2 $CHBrO + ClNO$	0.02499	−236.7	−234.5
P3 $CBrClO + HNO$	0.023678	−252.3	−253.4
IM1	0.028720	−215.6	−215.9
IM2	0.030871	−178.9	−177.5
IM3	0.028662	−206.6	−207.2
TS1	0.026465	86.5	87.3
TS2	0.027504	−171.9	−171.2
TS3	0.027365	−167.7	−168.1
TS4	0.023591	−105.3	−106.5
TS5	0.027301	−170.1	−171.1
TS6	0.027079	−147.0	−148.0
TS7	0.027028	−147.9	−149.5

through transition states TS3 and TS5, respectively. The dissociation barrier for IM1 → P1 and IM3 → P1 is 78.7 and 78.4 kJ/mol, respectively. Therefore, the three pathways are feasible, with the IM1 → TS3 → P1 pathway perhaps being favored by a very small degree. Both TS3 and TS5 present a loose $BrCO_1N$ four-membered ring structure, which is nonplanar. The corresponding forming Br–N bond lengths are 2.764 and 2.777 Å, while the breaking C–Br and O_1–N distances are 2.394 and 1.928 Å (in TS3), 2.329 and 1.895 Å (in TS5). The imaginary frequency of respective 233i and 187i mainly involves the simultaneous stretch vibrations of C–Br, O_1–N, and Br–N bonds. Alternatively, IM1 can take a 1, 3-H-shift and O_1–N bond rupture leading to product P2 CHBrO (C_s, $^1A'$) + HNO (C_s, $^1A'$) via TS4 or TS4′ with the barrier height 134.6 or 127.8 kJ/mol. The structures of TS4 and TS4′ are similar to each other and the obvious difference is caused by the dihedral angel $O_1H_2NO_2$ with 107.2° and −110.4°, respectively. The loose H_2CO_1N four-membered ring, which is slightly nonplanar, is found in TS4. The migrating hydrogen is 1.288 Å away from the origin (C atom) and 1.476 Å away from the migrating terminus (N atom), and the breaking O_1–N bond is surprisingly long as 2.189 Å. In addition, the primary product P1 can further dissociate to give P4 CH_2O (C_{2v}, $^2A1$) + Br + NO ($C_{\infty v}$, $^2\Pi$) via the direct N–Br single bond rupture. These processes can be simply described as:

$$\text{Path1}: \text{R} \rightarrow \text{IM1}, \text{IM3} \rightarrow \text{P1}(\text{CH}_2\text{O} + \text{BrNO}) \rightarrow \text{P4}(\text{CH}_2\text{O} + \text{Br} + \text{NO})$$

$$\text{Path2}: \text{R} \rightarrow \text{IM1} \rightarrow \text{P2}(\text{CHBrO} + \text{HNO})$$

Furthermore, isomer IM3 can undergo a 1,4-H-shift via TS6 and TS8 to form the isomers IM4 and IM5, respectively, which are *cis-trans* species for the HBrCONOH (C_s, $^1A'$) structure and can dissociate to give the product P3 CHBrO + HON (C_s, $^1A'$) via the transition states TS7 and TS9, respectively. These processes can simply be written as:

$$\text{Path3}: \text{R} \rightarrow \text{IM3} \rightarrow \text{IM4} \rightarrow \text{P3}(\text{CHBrO} + \text{HON})$$
$$\text{Path4}: \text{R} \rightarrow \text{IM3} \rightarrow \text{IM5} \rightarrow \text{P3}(\text{CHBrO} + \text{HON})$$

Because TS6, TS7, TS8 and TS9 are 39.5, 52.3, 31.7 and 34.8 kJ/mol higher than reactants R, respectively, the paths 3 and 4 are also kinetically less feasible at normal temperature and have negligible contributions to the $CH_2Br + NO_2$ reaction compared with the Paths 1 and 2.

Now, we turn our attention to the other isomerization and dissociation channels of the isomer IM2, as presented in Fig. A of Supplementary Material. First, a 1, 3-H shift-from C atom to O_2-atom associated with a concert twist of IM2 can form a1 or a3. Isomer a1 can readily convert to a2 via the N–O_2 single bond rotation transition state TSa1a2 with a small barrier of 2.5 kJ/mol, and the conversion of a3 → a2 is a process of C=N double bond rotations via the transition state TSa3a2 with the high barrier of 232.4 kJ/mol, while no transition state for the conversion of a1 → a3 was found. Because the a1 → a3 conversion involve a concerted process of C=N double bond and N–O_2 single bond simultaneous rotations, the high barrier may be faced for it. Subsequently, the ring-closure of a1, a2 and a3 may lead to the three-memberd ring isomer b (HBrC(O)-NOH) including b1, b2, b3, b4. Moreover, a3 can dissociate directly to give the product P5 BrCNO (C_s, $^1A'$) + H_2O (C_{2v}, $^2A1$) via side-H_2O cleavage. Such a process can be described as:

$$\text{Path5}: \text{R} \rightarrow \text{IM2} \rightarrow \text{a3} \rightarrow \text{P5}(\text{BrCNO} + \text{H}_2\text{O})$$

However, the conversion transition states TS10, TS11, TS12, TS13, TS14, TS15 and TS16 involved in IM2 → a1, a1 → b1, a2 → b2, IM2 → a3, a3 → b3, a3 → b4, and a3 → p5 conversion processes lie 48.5, 93.5, 97.3, 48.5, 122.7, 126.6 and 70.4 kJ/mol higher than the reactants R, respectively, as shown in Fig. 5 of Supplementary Material. Clearly, the formation Paths of a (a1, a2, a3), b (b1, b2, b3, b4) and P5 are less competitive than Paths 1 and 2 at room temperature.

3.1.3 Reaction mechanism

As presented in the preceding sections, we have obtained two important reaction channels (Paths 1–2) that are both thermodynamically and kinetically accessible for the singlet PES of $CH_2Br + NO_2$ reaction. The CH_2Br radical can barrierlessly react with NO_2 at the side-O site to form the low-lying adduct IM1 ($H_2BrCONO$-*trans*) and IM3 ($H_2BrCONO$-*cis*). Furthermore, isomer IM1 most favorably isomerizes to IM3 ($H_2BrCONO$-*cis*) involved in Path 1. Starting from IM1 and IM3, Path 1 leading to product P1 (CH_2O + BrNO) is more feasible than Path 2 starting from IM1 to form P2 (CHBrO + HNO) because the transition states TS3 (−144.6 kJ/mol) and TS5 (−141.9 kJ/mol) in Path 1 lie 55.9 and 53.2 kJ/mol lower than TS4 (−88.7 kJ/mol) in Path 2, respectively. When secondary dissociation procedure is considered, the direct N–Br single bond rupture of BrNO in P1 to form the secondary product P4 (CH_2O + Br +NO) may become possible after surmounting the dissociation barrier of 94.6 kJ/mol. Therefore, reflected in final product distributions, we predict that: (1) P1 may be the most feasible product with a largest yield; (2) P2 may be the second favorable products. (3) The primary product P1 (CH_2O + BrNO) can further dissociate to the secondary product P4 (CH_2O + Br + NO).

To further testify the reaction mechanism obtained at the UCCSD(T)//UB3LYP level, we performed additional UQCISD(T) single-point energy calculations for the most relevant species based on the UB3LYP/6-311G(d, p) geometries. As given in Table 3, the UQCISD(T)/6-311G(d, p) and UCCSD(T)/6-311G(d, p) level are in good agreement with each other. The largest deviation between the two levels is 4.6 kJ/mol for TS1. However, such discrepancies will not affect our discussion on the reaction mechanism. It is useful to make comparison for mechanism of the $CH_2Br + NO_2$ reaction between the UCCSD(T) and UQCISD(T) single-point levels. It is easily found from Table 3 that the features of PES obtained at the UQCISD(T)//UB3LYP level are in general consistent with that at the UCCSD(T)//UB3LYP level. (1) Paths 1 and 2 are both thermodynamically and kinetically feasible channels. (2) Most importantly, the high level calculations predict that Path 1 is more competitive than Path 2 because the relative energies of TS3 and TS5 in Path 1 are lower than that of TS4 in Path 2 and product P1 (−227.1 kJ/mol) is a little stabler than P2 (−222.8 kJ/mol).

3.2 Reaction CHBrCl + NO_2

3.2.1 Isomerization and dissociation pathways

On the singlet PES of CHBrCl + NO_2 reaction, the carbon-to-oxygen approach is rather attractive to form IM1 (HBrClCONO-*trans*) and IM3 (HBrClCONO-*cis*) without any encounter barrier. For the carbon-to-nitrogen attack, we locate the weak bond complex IM2 ($HBrClCNO_2$) with the energy −178.9 kJ/mol. The energy of IM1 and IM3 are −215.6 and −206.6 kJ/mol lower than the reactants R, respectively, as shown in Fig. 4. Thus, the complexes IM1 and IM3 could be most likely formed initially from the energy point of view. On the other hand, on the triplet PES of CHBrCl + NO_2 reaction, there is a substantial barrier of 98.0 kJ/mol (^{3}TSRIM1) for the carbon-to-oxygen attack to form isomer ^{3}IM1 (HBrClCONO-*trans*, 91.6 kJ/mol), and the carbon-to-nitrogen approach can be realized via ^{3}TSRIM2 with a barrier of 155.4 kJ/mol leading to the chainlike isomer ^{3}IM2 ($HBrClCNO_2$), which is 69.7 kJ/mol

higher than the reactants R. It is clear that the triplet pathways should be much less competitive than the singlet pathways due to the high barrier height. Thus, for the $CHBrCl + NO_2$ reaction, the exclusive feasible entrance channels are the barrierless O atom of NO_2 attacked by C atom of CHBrCl to form IM1 and IM3 on the singlet PES. The isomer IM1 may undergo C–N bond formation and C–O bond rupture via TS1 leading to IM2. Note that the IM1 → IM2 conversion barrier (TS1) is rather high as 302.1 kJ/mol and TS1 lies 86.5 kJ/mol higher than the reactants R. Thus, this conversion process is very difficult to occur. On the other hand, IM1 can easily convert to IM3. The conversion from IM1 to IM3 can be realized via O_1–N bond rotation transition state TS2 with a small internal rotation barrier (43.7 kJ/mol above IM1). Subsequently, intermediate IM3 can dissociate to give the primary product P1 (CHClO + BrNO) via TS5. Furthermore, isomers IM1 and IM3 can directly dissociate to give the primary products P1 (CHClO + BrNO) and P2 (CHBrO + ClNO) via C–Br, C–Cl and N–O_1 bonds cleavage accompanied by N–Br and N–Cl bonds formation through transition states TS3, TS6 and TS5, TS7, respectively. Only the 47.9 (TS3 for IM1), 68.6 (TS5 for IM1), 36.5 (TS6 for IM3) or 58.7 (TS7 for IM3) kJ/mol barrier is needed to overcome for these processes. The direct N–Br and N–Cl single bonds rupture of BrNO and ClNO in P1 and P2 to form the secondary products P5 (CHClO + Br + NO) and P6 (CHBrO + Cl + NO) may be possible after surmounting the dissociation barrier of 94.6 and 58.3 kJ/mol, respectively. These processes can simply be written as:

$$\begin{aligned}\text{Path1}: \mathrm{R} &\rightarrow \mathrm{IM1}, \mathrm{IM3} \rightarrow \mathrm{P1}(\mathrm{CHClO} + \mathrm{BrNO}) \\ &\rightarrow \mathrm{P5}(\mathrm{CHClO} + \mathrm{Br} + \mathrm{NO})\end{aligned}$$

$$\begin{aligned}\text{Path2}: \mathrm{R} &\rightarrow \mathrm{IM1}, \mathrm{IM3} \rightarrow \mathrm{P2}(\mathrm{CHBrO} + \mathrm{ClNO}) \\ &\rightarrow \mathrm{P6}(\mathrm{CHBrO} + \mathrm{Cl} + \mathrm{NO})\end{aligned}$$

Furthermore, the isomer IM1 can take a 1, 3-H-shift and O_1–N bond ruptures leading to P3 CHBrCl + HNO via TS4, and the dissociation barrier is 110.3 kJ/mol. The formation pathway of P3 is:

$$\text{Path3}: \mathrm{R} \rightarrow \mathrm{IM1} \rightarrow \mathrm{P3}(\mathrm{CBrClO} + \mathrm{HNO})$$

Alternatively, isomer IM3 (HBrClCONO-*cis*) can undergo a 1, 4-H-shift from C to O atom to form IM4 (BrClCONOH) via TS8 with the barrier height of 258.9 kJ/mol. Isomer IM4 can directly dissociate to N–O_1 to form product P4 (CBrClO + HON). Note that we have tried to search for the N–O_1 bond cleavage transition state at UB3LPY/6-311G(d, p) level, yet with no success. But we expect that IM4 could dissociate to (CBrClO + HON) via a simple N–O_1 bond fission without a pronounced barrier as in the case of the reaction of $CH_2Br + NO_2$. The formation pathway of P4 is:

$$\text{Path4}: \mathrm{R} \rightarrow \mathrm{IM3} \rightarrow \mathrm{IM4} \rightarrow \mathrm{P4}(\mathrm{CBrClO} + \mathrm{HON})$$

Now, we turn our attention to the other isomerization and dissociation channels of the isomer IM2 ($HBrClCNO_2$). The optimized structures are shown in Fig. 6 in the Supplementary Material. a1, a2, a3, and a4 are *cis-trans* isomers for the BrClCN(O)OH structure in terms of C-bound bromine or O-bound hydrogen. First, a 1, 3 H-shift from C atom to O_2-atom associated with a concert twist of IM2 can form a1 (BrClCN(O)OH) or a3. Isomer a1 and a3 can readily convert to a2 and a4 via the N–O_2 single bond rotation transition states TSa1a2 and TSa3a4, respectively. Then, the ring-closure of a (a1, a2, a3, a4) may lead to the three-membered ring isomer b (b1, b2, b3, b4). However, the conversion transition states TS10, TS11, TSa1b1, TSa2b2, TSa3b3, TSa4b4 involved in a1 → b1, a2 → b2, a3 → b3, and a4 → b4 conversion processes lie 57.4, 57.4, 108.8, 85.1, 110.9, 90.2 kJ/mol higher than the reactants, respectively. Clearly, the formation of a (a1, a2, a3, a4) and b (b1, b2, b3, b4) are less competitive than Paths 1 and 2 at room temperature.

3.2.2 Reaction mechanism

In the previous sections, we have obtained three important reaction channels (Path 1–3) for the $CHBrCl + NO_2$ reaction. The CHBrCl radical can barrierlessly react with NO_2 at the side-O site to form the low-lying adduct IM1 (HBrClCONO-*trans*) and IM3 (HBrClCONO-*cis*). The most competitive pathway should be Path 1 leading to product P1 (CHClO + BrNO) due to the least reaction steps and lowest overall barriers from the common intermediate IM3 to the final dissociation products. There are three possible channels in Path 1. Note that it may be difficult to differentiate among the three possible channels with certainty from the data of barrier height, with the IM3 → TS5 → P1 pathway perhaps being favored by a very small degree. Furthermore, Path 2 and Path 3 may be kinetically the second and third feasible pathways, because starting from IM1 and IM3, the relative energy of the associated rate-determining transition states TS6 (−147.0 kJ/mol) and TS7 (−147.9 kJ/mol) in Path 2 lie 41.7 and 42.6 kJ/mol lower than TS4 (−105.3 kJ/mol) in Path 3, respectively. When secondary dissociation procedures are considered, the primary products P1 and P2 will lead to P5 (CHClO + Br + NO) and P6 (CHBrO + Cl + NO), respectively. As a result, reflected in the final product distribution, we predict that the primary P1 (CHClO + BrNO) is kinetically the most feasible product. P2 and P3 may be the second and third favorable products. The secondary products P5 and P6 may occupy only a small part.

Furthermore, we also performed additional UQCISD(T) and UCCSD(T) single-point energy calculations for some important stationary points based on UB3LYP/6-311G(d, p) optimized geometries. As shown in Table 4, the UQCISD(T) and UCCSD(T) single-point energies are generally in good agreement with each other with the large deviation lies in P2 only 2.2 kJ/mol.

3.3 Experimental implications

Our results are in good agreement with kinetic study results by Timonen et al. [14]. For the $CH_2Br + NO_2$ reaction, the observed major product is CH_2O, which can be found as one species of the most favorable product P1 ($CH_2O + BrNO$) in our calculations. Formation of NO was also detected, but because of the production of radicals other than CH_2Br in the photolysis or in the secondary chemistry and their possible reactions with NO_2 to produce NO, it was impossible to assign the origin of NO unambiguously to the $CH_2Br + NO_2$ reaction in Timonen et al.'s experiment. While, based on our present calculations, we make sure that the further dissociation of BrNO in primary P1 can produce species NO. For the $CHBrCl + NO_2$ reaction, the detected product CHClO has indeed been identified in our calculations (denoted as one species in P1 (CHClO + BrNO)), and the further dissociation of BrNO in P1 can produce NO. Timonen et al. [14] stated that "For the reactions $CH_2Br + NO_2$ and $CHBrCl + NO_2$ other potential products that were searched for but not observed." Therefore, further kinetic investigations are still required for the unobserved products BrNO, CHBrO, Br, HNO for $CH_2Br + NO_2$ reaction and BrNO, CBrClO, Br, Cl, HNO, CHBrO, and ClNO for $CHBrCl + NO_2$ reaction to deeply understand the mechanism of the title reactions. In addition, the reactions of $CH_2Br + NO_2$ and $CHBrCl + NO_2$ are expected to contribute to the elimination of nitrogen dioxide pollutants and may be of significance in atmospheric chemistry.

3.4 Comparison between the reactions of CH_2Br and CHBrCl with NO_2

It is of interest to compare the potential energy surface feature of the $CH_2Br + NO_2$ reaction with the $CHBrCl + NO_2$ one. By comparison, it is readily found that the features of potential energy surfaces on the $CHXBr + NO_2$ (X=H and Cl) reactions are almost in parallel. The reaction pathways leading to the feasible products (including the secondary dissociation pathways) can be summarized as:

$$\text{Path1}: CHBrX + NO_2 \rightarrow HBrXCONO \rightarrow CHXO + BrNO$$

$$\text{Path2}: CHBrX + NO_2 \rightarrow HBrXCONO - \textit{trans} \rightarrow CBrXO + HNO$$

$$\text{Path3}: CHBrX + NO_2 \rightarrow HBrXCONO - \textit{cis} \rightarrow BrXCONOH \rightarrow CBrXO + HON$$

$$\text{Path4}: CHBrCl + NO_2 \rightarrow HBrClCONO \rightarrow CHBrO + ClNO$$

As we can see, all these four pathways involve the same side-O association process $CHBrX + NO_2 \rightarrow HBrXCONO$ (X=H and Cl). For the two reactions, isomers HBrXCONO (X=H and Cl) can undergo 1,3-bromine migration from C to N atom associated with $N–O_1$ weak bond cleavage leading to species CHXO (X=H and Cl) + BrNO as the most favorable product. The primary product CBrXO + HNO (X=H and Cl) can be obtained for both reactions $CH_2Br + NO_2$ and $CHBrCl + NO_2$. The product CBrXO + HON (X=H and Cl) can also be obtained for both reactions and it has less contribution to both reactions. However, some quantitative discrepancy leads to the different product distribution for the two reactions. For the $CH_2Br + NO_2$ reaction, the most feasible product is $CH_2O + BrNO$ (via Path 1) and the second feasible product is CHBrO + HNO (via Path 2) with a comparable yield, followed by CHBrO + HON (via Path 3) is the least competitive product. For the $CHBrCl + NO_2$ reaction three kinds of products can be formed that is, CHClO + BrNO (via Path 1), CHBrO + ClNO (via Path 4), CBrClO + HNO (via Path 2). The order of their feasibility should be CHClO + BrNO > CHBrO + ClNO > CBrClO + HNO. In addition, the products CHClO + BrNO and CHBrO + ClNO can further dissociate to give species CHClO + Br + NO and CHBrO + Cl + NO, respectively.

4 Conclusions

The mechanistic studies of the CH_2Br, $CHBrCl + NO_2$ reaction systems have been carried out theoretically as an attempt to understand the halogenated methyl chemistry. The detailed singlet potential energy surface including 24 isomers and 34 transition states was established at the UB3LYP and UCCSD(T) (single-point) levels. The mechanism can generally be summarized as association, isomerization, and dissociation processes.

(1) For the $CH_2Br + NO_2$ reaction, the C atom of CH_2Br radical can barrierlessly attack the O atom of NO_2 to form the initial radical-molecular adduct IM1 (H_2BrC-ONO-*trans*) and IM3 ($H_2BrCONO$-*cis*). Starting form

IM1, two primary products P1 (CH_2O + BrNO) and P2 (CHBrO + HNO), and one secondary product P5 (CH_2O + Br + NO) should be observed. P2 is the less feasible product. Our results agree well with the experimental observation for $CH_2Br + NO_2$ reaction.

(2) For the $CHBrCl + NO_2$ reaction, three kinds of primary products P1 (CHClO + BrNO), P2 (CHBrO + ClNO) and P3 (CBrClO + HNO) should be observed. Among these products, P1 is the most favorable product while P2 and P3 are second and third feasible products, respectively. In addition, P5 (CHClO + Br + NO) and P6 (CHBrO + Cl + NO) as kinetically accessible secondary products may have a small amount.

(3) The PES features of the $CH_2Br + NO_2$ and $CHBrCl + NO_2$ reactions are similar. The triplet pathways have much less competitive abilities for both reactions and can thus be neglected. The present theoretical studies may provide useful information on the reaction mechanism and assist in further laboratory identification of the products for the title reactions.

Acknowledgments This work is supported by the National Natural Science Foundation of China (No. 20773021), the Science Foundation for Young Teachers of Northeast Normal University (No. 20070315), and Training Fund of NENU'S Scientific Innovation Project (NENU-STC07016). We are greatly thankful for the referees' helpful comments.

References

1. Baren RE, Erickson M, Hershberger JF (2002) Int J Chem Kinet 34:12. doi:10.1002/kin.10013
2. Rim KT, Hershberger JF (1998) J Phys Chem A 102:4592. doi:10.1021/jp981362k
3. Lanier WS, Mulholland JA, Beard JT (1988) Symp Int Combust Proc 21:1171
4. Chen SL, McCarthy JM, Clark WD, Heap MP, Seeker WR, Pershing DW (1988) Symp Int Combust Proc 21:1159
5. Carpenter LJ, Liss PS, Penkett SA (2003) J Geophys Res 108:4256. doi:10.1029/2002JD002769
6. Jordan A, Harnisch J, Borchers R, le Guern F, Shinohara H (2000) Environ Sci Technol 34:1122. doi:10.1021/es990838q
7. Bilde M, Wallington TJ, Ferronato C, Orlando JJ, Tyndall GS, Estupiñan E, Haberkorn S (1998) J Phys Chem A 102:1976. doi:10.1021/jp9733375
8. Mellouki A, Talukdar RK, Schmoltner AM, Gierczak T, Mills MJ, Solomon S, Ravishankara AR (1992) Geophys Res Lett 19:2059. doi:10.1029/92GL01612
9. Tzima TD, Papavasileiou KD, Papayannis DK, Melissas VS (2006) Chem Phys 324:591. doi:10.1016/j.chemphys.2005.11.021
10. Pfeilsticker K, Sturges WT, Bösch H, Camy-Peyret C, Chipperfield MP, Engel A, Fitzenberger R, Müller M, Payan S, Sinnhuber BM (2000) Geophys Res Lett 27:3305. doi:10.1029/2000GL011650
11. Schauffler SM, Atlas EL, Blake DR, Flocke F, Lueb RA, Lee-Taylor JM, Stroud V, Travnicek W (1999) J Geophys Res 104(17):513. doi:10.1029/1999JD900197
12. Faravelli T, Frassoldati A, Ranzi E (2003) Combust Flame 132:188. doi:10.1016/S0010-2180(02)00437-6
13. Eskola AJ, Geppert WD, Rissanen MP, Timonen RS, Halonen L (2005) J Phys Chem A 109:5376. doi:10.1021/jp050441a
14. Eskola AJ, Pastuszka DW, Ratajczak E, Timonen RS (2006) J Phys Chem A 110:12177. doi:10.1021/jp064197e
15. Zhang JX, Li ZS, Liu JY, Sun CC (2005) J Comput Chem 27:661. doi:10.1002/jcc.20380
16. Zhang JX, Li ZS, Liu JY, Sun CC (2005) J Comput Chem 27:894. doi:10.1002/jcc.20397
17. Zhang JX, Li ZS, Liu JY, Sun CC (2007) Theor Chem Acc 117:579. doi:10.1007/s00214-006-0244-8
18. Frisch MJ, Trucks GW, Schlegel HB et al (2004) Gaussian 03, revision C.02. Gaussian, Inc., Wallingford
19. Becke AD (1993) J Chem Phys 98:5648. doi:10.1063/1.464913
20. Lee C, Yang W, Parr RG (1988) Phys Rev B 37:785. doi:10.1103/PhysRevB.37.785
21. Pople JA, Head-Gordon M, Raghavachari K (1987) J Chem Phys 87:5968. doi:10.1063/1.453520
22. Gonzalez C, Schlegel HB (1989) J Chem Phys 90:2154. doi:10.1063/1.456010
23. Gonzalez C, Schlegel HB (1990) J Phys Chem 94:5523. doi:10.1021/j100377a021
24. Kuchitsu K (1998) Structure of free polyatomic molecules basic data. Springer, Berlin
25. Lide DR (1999) CRC handbook of chemistry and physics, 80th edn. CRC Press, Boca Raton
26. In NIST Chemistry WebBook. NIST standard reference database number 69, June (2005) release (vibrational frequency data compiled by Jacox. M. E)